Physical Optics Analysis of a Four-Reflector Antenna Part 2

A. G. Cha
Radio Frequency and Microwave Subsystems Section

The results of a rigorous analysis of the DSN 70-m antenna S-band (2.295-GHz) RF performance are presented. Previous estimation of 1.6 dB S-band gain improvement of the 70-m antenna over the 64-m antenna has been revised to 1.5 dB by this analysis. The S-band RCP beam position offset relative to X-band (8.45-GHz) beam position is predicted to be 0.0045° (0.04 beamwidth). The effective S-band gain loss resulting from non-coincidence with the X-band beam is predicted to be 0.02 dB. Therefore, this is no longer a concern for the 64-m to 70-m upgrade project.

I. Introduction

The initial configuration of the DSN 70-m antennas, shown in Fig. 1, will retain the present 64-m S/X band (2.295/8.45 GHz) reflex dichroic feed system, but will replace the hyperboloid subreflector and parabolic main reflector by an asymmetric shaped subreflector and a symmetric shaped main reflector. In Part 1 of this article (Ref. 1), the 64-m antenna four-reflector S-band system was analyzed using a rigorous physical optics (PO) based procedure; theoretical predictions were found to be in excellent agreement with known 64-m antenna experimental information. The same analysis procedure is now applied to the 70-m shaped antenna four-reflector S-band system.

In Part 1 of this article, the NASA/JPL 64-m antenna RF performance was analyzed at S-band (2.295 GHz) using a rigorous physical optics approach. Excellent agreement with all known 64-m experimental characteristics was achieved, establishing the analysis procedure as a valid tool for predicting RF performance in arbitrary multiple reflector antenna systems. In this article, the same approach is extended to analyzing the S-band performance for the upcoming 70-m antenna conversion, with particular interest in determining the S-band beam pointing direction. The uncertainty in S-band performance associated with the uncertainty of S-band beam position had prompted this study.

II. Comparisons of Diffraction and Polarization Characteristics for 64-m Classical Cassegrain vs 70-m Dual-Shaped Subreflectors

In Figs. 2 through 4, the 2.295-GHz diffraction patterns of the ellipsoid subreflector, the dichroic plate, the 64-m hyperboloid, and the 70-m asymmetric subreflector are shown. The ellipsoid E- and H-plane diffraction patterns have a small but observable asymmetry compared to the incident corrugated horn patterns. (The corrugated horn patterns are not shown but exhibit perfect E- and H-plane symmetry.) The ellipsoid diffraction pattern asymmetry is a manifestation of the presence of higher order azimuthal Fourier modes induced by

the asymmetric geometry of the horn and ellipsoid. This moding effect is the primary factor causing S-band (2.295-GHz) beam pointing direction of the 64-m and 70-m antennas to be polarization dependent (and to be offset from the X-band (8.45-GHz) beam pointing direction). The dichroic diffraction pattern is substantially the same as the ellipsoid diffraction pattern, as one would expect from a planar reflector. The hyperboloid diffraction patterns shown in Fig. 3 correspond to the 64-m subreflector, less its flange. As noted in Part 1, the flange is not expected to have any significant effect in beam pointing direction prediction. The hyperboloid diffraction pattern exhibits a tapered illumination from main reflector axis ($\theta = 0^\circ$) to optical edge ($\theta = 60^\circ$). By contrast, the 70-m antenna shaped subreflector diffraction patterns shown in Fig. 4 show the expected inverse illumination taper, which is needed to realize nearly uniform aperture illumination for high aperture efficiency. The center dip in the pattern (approximately, polar angle = 0° to 10° in Fig. 4) is due to a "vertex plate" design, which is estimated to improve 70-m S- and X-band gain by more than 0.1 dB.

Each diffraction pattern has been analyzed by a Fourier series expansion analysis to determine its azimuthal Fourier modes (*m*-modes) power content. This is shown in Fig. 5 and Table 1. It is well known that only the m = 1 mode contributes to antenna boresight gain, while the $m \neq 1$ modes lead to gain loss and cross-polarization radiation. The reference for viewing the mode content of each diffraction pattern is the corrugated horn pattern illuminating the ellipsoid. For most practical purposes, nearly 100% of the power radiated by the corrugated horn is in the m = 1 mode. After reflection from the ellipsoid, it is seen that about 2% of the power is converted into the m = 0 and m = 2 modes. The dichroic reflector diffraction pattern and mode power contents are essentially the same as those of the ellipsoid. Both the 64-m antenna hyperboloid and the 70-m antenna shaped subreflector are illuminated by the dichroic diffraction pattern. Although the two subreflector diffraction patterns, Figs. 3 and 4, look drastically different, the amount of power in the undesirable higher order m modes is approximately the same (3%) in both cases.

The computed 70-m S-band (2.295-GHz) far-field radiation pattern is shown in Tables 2 and 3 in two perpendicular planes (defined as $\phi = 180^\circ$ and 270°). Similar to the 64-m antenna case presented in Part 1, beam position offsets in these two planes correspond respectively to the 2.54-cm (1-in.) shim of the dichroic position and the depolarization effect of the $m \neq 1$ modes on circularly polarized waves (RCP in the present case). Figure 6 shows the predicted 70-m antenna S-band beam position relative to the known 64-m antenna X- (8.45-GHz) and S-band positions. The beam position offset in the $\phi = 270^\circ$ plane is approximately the beam separation between the X- and S-band beams. This is computed to be 0.0045° (equal to 4% of the 70-m antenna S-band beamwidth). Assuming the antenna is boresighted by the X-band beam, an S-band equivalent pointing loss of 0.02 dB is to be expected.

The 70-m antenna S-band (2.295-GHz) beam position offset calculated above is considerably smaller than that observed in or calculated for the 64-m antenna (0.0086° or 6.1% beamwidth observed, 0.0095° or 6.8% beamwidth calculated). Although this comes somewhat as a surprise, the results appear reasonable from the following consideration. Figure 7 shows an aperture with a linear phase gradient. The aperture phase is $(-)\Phi_{AP}$ at $x = -D/2$, and increases linearly to $+\Phi_{AP}$ at $x = +D/2$. The beam offset angle θ from aperture normal is then

$$\theta = \frac{\lambda \Phi_{AP}}{\pi D} \tag{1}$$

where λ is the wavelength.

From Eq. (1), one can attribute the smaller beam offset partly to the larger diameter of the 70-m antenna. It is further expected that the aperture edge phase deviation Φ_{AP} would also be smaller in the 70-m case. The aperture edge phase deviation Φ_{AP} is approximately

$$\Phi_{AP} = \tan^{-1}\left|\frac{E_c}{E_p}\right| \tag{2}$$

where E_c and E_p are fields arising from the $m \neq 1$ modes and m = 1 mode near the aperture edge, respectively. From Table 1, we see the higher order mode energy in both cases is mostly in the m = 2 component. For a qualitative argument, we assume E_c to be $E_{m=2}$, and also that E_c is approximately the same for both antennas. However, E_p should be larger at the aperture edge for the uniformly illuminated 70-m antenna than for the 64-m antenna with highly tapered illumination. We can therefore expect Φ_{AP} to be smaller in the 70-m case, further reducing the offset angle θ from boresight, Eq. (1).

III. 70-m Antenna S-Band RF Performance

The 70-m antenna S-band (2.295-GHz) theoretical performance was previously estimated based on a two-reflector, tricone feed geometry system.[1] The two-reflector analysis

[1] Cha, A. G., *Physical Optics Analysis of NASA/JPL Deep Space Network 70-m Antennas* (JPL Internal Document D-1853), Jet Propulsion Laboratory, Pasadena, CA, Nov. 1984.

results were modified based on the best information then available as to what the effects of the two additional subreflectors (the ellipsoid and the dichroic plate) would be in the overall four-reflector system. The baseline 64-m antenna S-band performance used in deriving the performance improvement of the 70-m over the 64-m antenna was based on Ref. 2. The estimated S-band performance improvement was 1.6 dB, from area enlargement and RF optics improvement. It was recognized that there were two significant approximations involved in the above derivation of the 1.6-dB performance improvement. First, the 70-m analysis was not a real four-reflector analysis. Second, the 64-m and 70-m performance values were not derived on the same computational bases and could therefore involve bias errors when the two sets of performance data are used to predict the performance improvement. The present four-reflector S-band analysis of the 64-m and 70-m antennas eliminates both of the above approximations and their associated errors. Based on the four-reflector analysis, S-band gain values for 70-m and 64-m antennas are 63.97 dB and 62.45 dB, respectively. These values include losses due to spillovers, non-uniform amplitude and phase in aperture illumination, $m \neq 1$ modes, crosspolarization-equivalent pointing loss from S-band beam position shift, and central blockage. The revised 70-m over 64-m performance values are shown in Fig. 8. The theoretical S-band performance improvement due to area and RF optics is seen to be 1.5 dB, which is 0.1 dB below the earlier estimate but still 0.1 dB over project requirements. There is no revision on X-band (8.45-GHz) performance improvement, which is shown for reference. In addition, there should be some gain improvement due to reduced quadripod blockage. (This is shown as a 0.0 to +0.3 dB uncertainty in Fig. 8.)

References

1. Cha, A. G., "Physical Optics Analysis of a Four-Reflector Antenna: Part 1," *TDA Progress Report 42-84*, pp. 94–100, Jet Propulsion Laboratory, Pasadena, CA, Feb. 15, 1986.

2. Bathker, D. A., "Dual-Frequency Dichroic Feed Performance," presented at 26th Meeting of Avionics Panel, AGARD, Munich, Germany, November 26–30, 1973, *AGARD Conference Proceedings #139*, June 1974, NATO.

Table 1. Azimuthal Fourier mode power content of subreflector diffraction patterns

m	Mode Power as Percent of Total Power			
	22-dB Horn	Ellipsoid or Dichroic	64-m Hyperboloid	70-m Shaped Subreflector
0	~0.0	0.9	0.6	1.1
1	~100.0	98.1	97.1	97.0
2	~0.0	0.9	2.3	1.8
3	~0.0	<0.1	<0.1	<0.1

Table 2. Beam offset caused by 2.54-cm (1-in.) shim of dichroic position[a]

Theta	E Theta		E Phi		Axial Ratio	Ellipse Tilt Angle	RCP Gain, dB
	Volts	Phase	Volts	Phase			
0.00000	176.583868	87.147	176.457674	2.850	0.006	1.99780	63.953
0.00100	176.871906	87.088	176.736952	2.912	0.007	0.22150	63.967
0.00200	177.124393	87.029	176.981068	2.973	0.007	178.63421	63.979
0.00300	177.341164	86.970	177.189932	3.034	0.007	177.19939	63.989
0.00400	177.522308	86.912	177.363615	3.095	0.008	175.89006	63.998
0.00500	177.667601	86.854	177.501917	3.156	0.008	174.68122	64.005
0.00600	177.777067	86,796	177.604851	3.217	0.009	173.55564	64.010
0.00700	177.850657	86,738	177.672361	3.278	0.009	172.49714	64.014
0.00800[b]	177.888355	86.680	177.704437	3.338	0.009	171.49430	64.015
0.00900[b]	177.890163	86.622	177.701069	3.398	0.010	170.53761	64.015
0.01000	177.856033	86.565	177.662327	3.459	0.010	169.61446	64.014
0.01100	177.786058	86.508	177.588160	3.519	0.010	168.72233	64.010
0.01200	177.680252	86.450	177.478649	3.579	0.011	167.85401	64.005
0.01300	177.538679	86.393	177.333836	3.639	0.011	167.00534	63.998
0.01400	177.361317	86.339	177.153761	3.696	0.011	166.16812	63.989
0.01500	177.148457	86.282	176.938639	3.756	0.012	165.34344	63.979
0.01600	176.900034	86.225	176.688459	3.816	0.012	164.52626	63.966
0.01700	176.616140	86.169	176.403273	3.875	0.012	163.71426	63.952
0.01800	176.296972	86.113	176.083372	3.934	0.013	162.90046	63.937
0.01900	175.942684	86.056	175.728769	3.994	0.013	162.09123	63.919
0.02000	175.553347	86.001	175.339638	4.053	0.013	161.27848	63.900

[a]Plane $\phi = 180°$ (direction of 0.0114° beam offset, see Fig. 6).
[b]Beam position for peak gain.

Table 3. Offset of right circularly polarized beam from antenna boresight [a]

Theta	E Theta		E Phi		Axial Ratio	Ellipse Tilt Angle	RCP Gain, dB
	Volts	Phase	Volts	Phase			
0.00000	176.457674	2.850	176.583868	92.853	0.006	1.99475	63.953
0.00100	176.593958	2.909	176.726660	92.914	0.007	3.23790	63.960
0.00200	176.694437	2.968	176.834131	92.975	0.007	4.35443	63.965
0.00300	176.759111	3.026	176.906185	93.035	0.007	5.35418	63.968
0.00400[b]	176.787991	3.084	176.942875	93.095	0.008	6.24177	63.970
0.00500[b]	176.781010	3.141	176.944080	93.154	0.008	7.02990	63.970
0.00600	176.738192	3.198	176.909853	93.214	0.009	7.72686	63.968
0.00700	176.659531	3.255	176.840151	93.273	0.009	8.34092	63.964
0.00800	176.545029	3.311	176.735043	93.331	0.010	8.87782	63.959
0.00900	176.394760	3.368	176.594500	93.390	0.010	9.35170	63.952
0.01000	176.208757	3.423	176.418629	93.448	0.011	9.76480	63.943
0.01100	175.987118	3.479	176.207468	93.505	0.012	10.12679	63.932
0.01200	175.729912	3.534	175.961098	93.563	0.012	10.44147	63.920
0.01300	175.437237	3.589	175.679642	93.620	0.013	10.71383	63.905
0.01400	175.109095	3.641	175.363056	93.675	0.014	10.94936	63.889
0.01500	174.745895	3.695	175.011717	93.731	0.014	11.15447	63.872
0.01600	174.347519	3.749	174.625599	93.787	0.015	11.32791	63.852
0.01700	173.914185	3.802	174.204796	93.843	0.016	11.47777	63.831
0.01800	173.446131	3.856	173.749630	93.899	0.017	11.60288	63.808
0.01900	172.943472	3.909	173.260151	93.954	0.017	11.70823	63.783
0.02000	172.406422	3.961	172.736588	94.009	0.018	11.79514	63.756

[a]Plane $\phi = 270°$ (direction of 0.0086° beam offset, see Fig. 6).
[b]Beam position for peak gain.

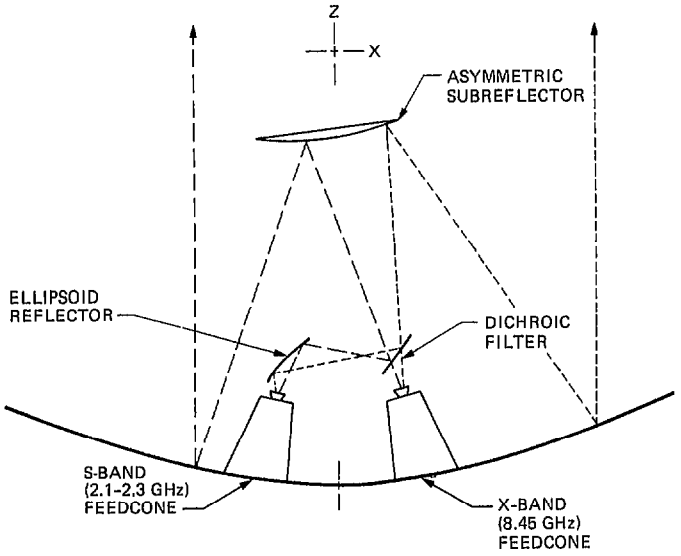

Fig. 1. 70-m antenna four-reflector geometry

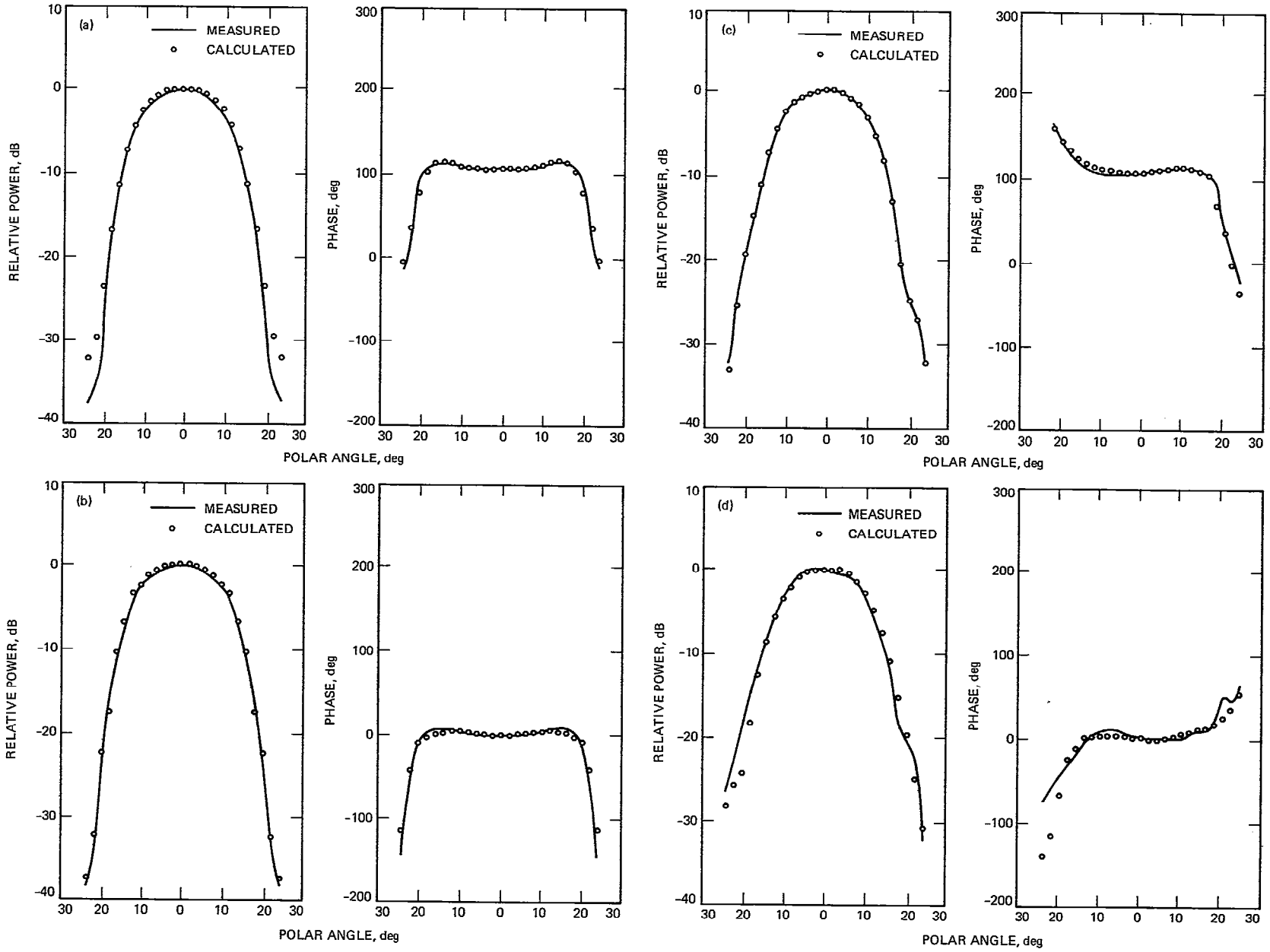

Fig. 2. Ellipsoid and dichroic diffraction patterns: (a) ellipsoid E-plane; (b) dichroic E-plane; (c) ellipsoid H-plane; (d) dichroic H-plane

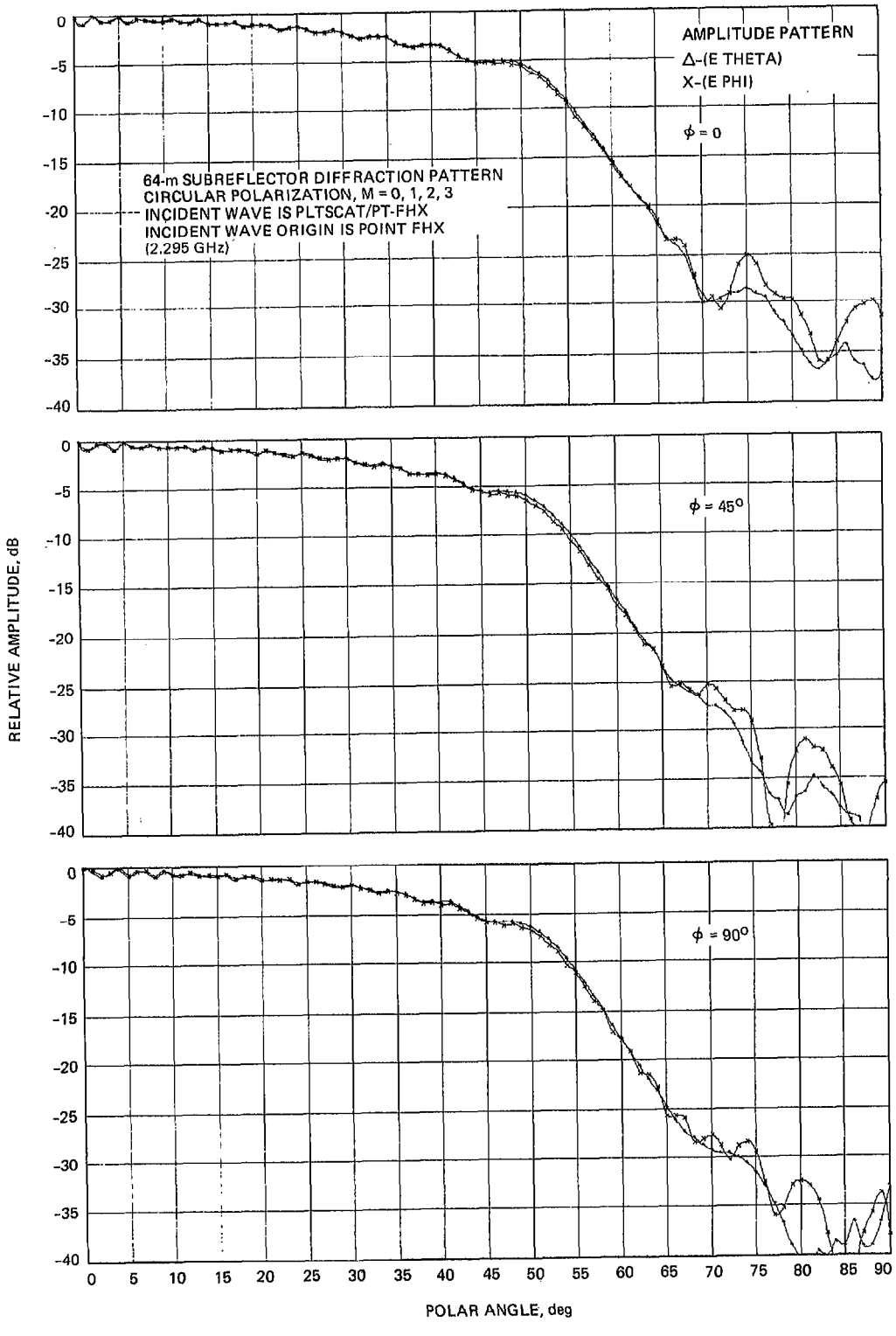

Fig. 3. 64-m hyperboloid diffraction patterns

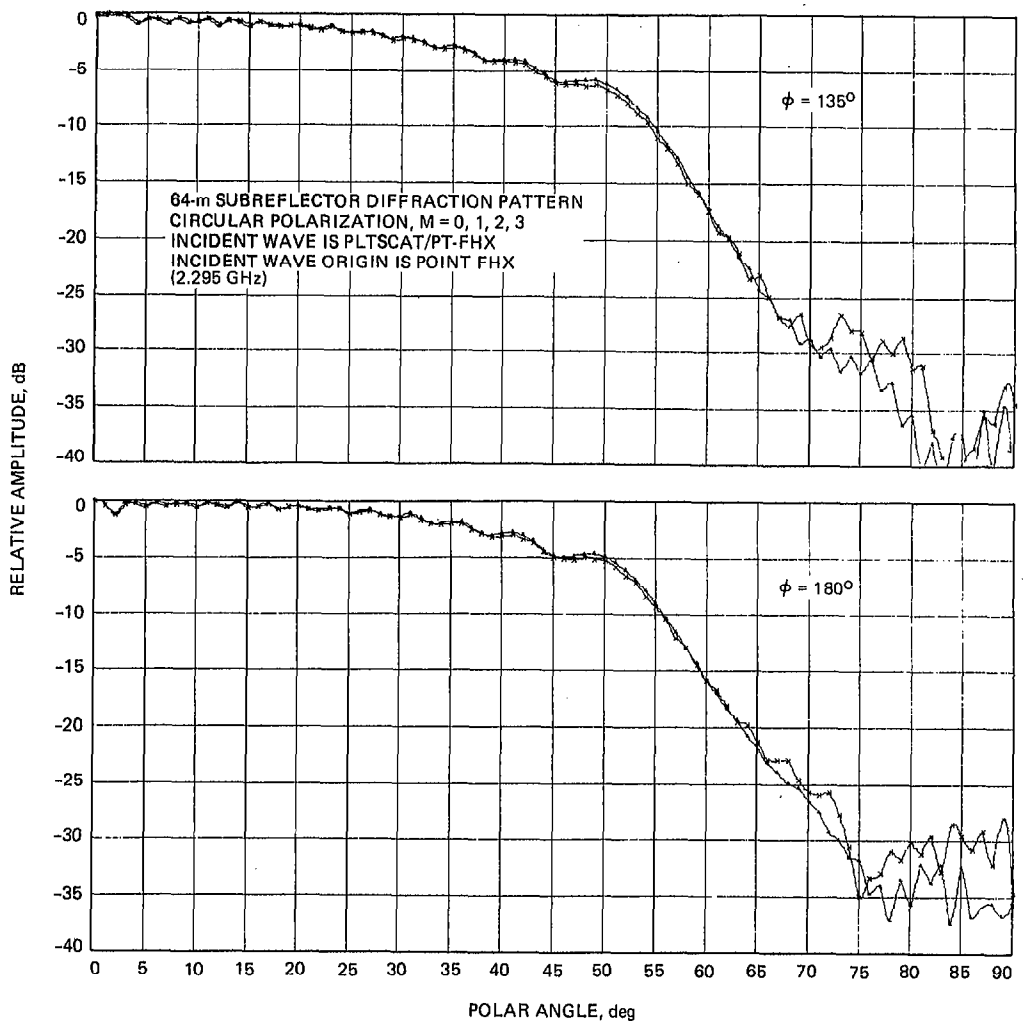
64-m SUBREFLECTOR DIFFRACTION PATTERN
CIRCULAR POLARIZATION, M = 0, 1, 2, 3
INCIDENT WAVE IS PLTSCAT/PT-FHX
INCIDENT WAVE ORIGIN IS POINT FHX
(2.295 GHz)
ϕ = 135°
ϕ = 180°
RELATIVE AMPLITUDE, dB
0
-5
-10
-15
-20
-25
-30
-35
-40
0 5 10 15 20 25 30 35 40 45 50 55 60 65 70 75 80 85 90
POLAR ANGLE, deg

Fig. 3 (contd)

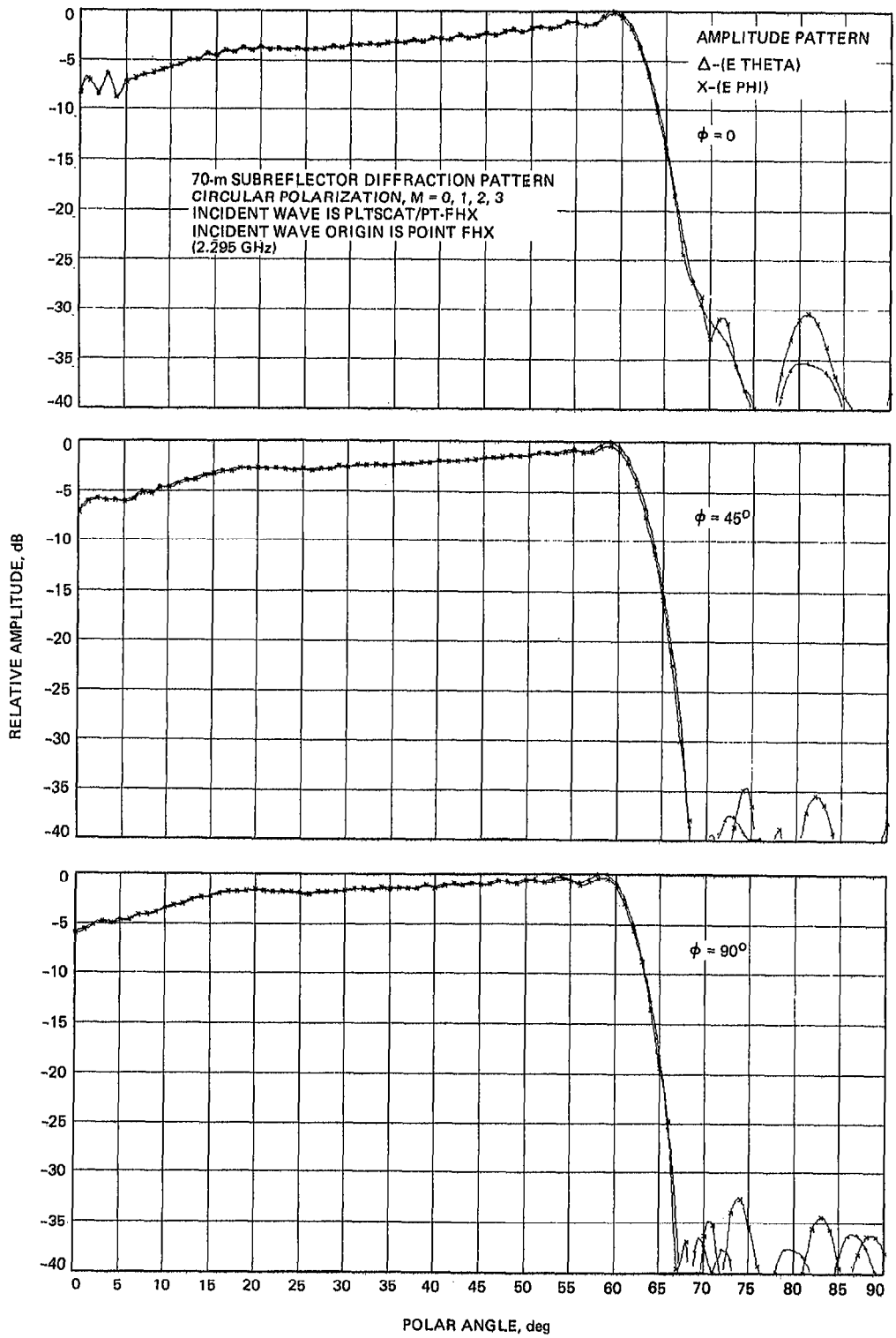

Fig. 4. 70-m shaped subreflector diffraction patterns

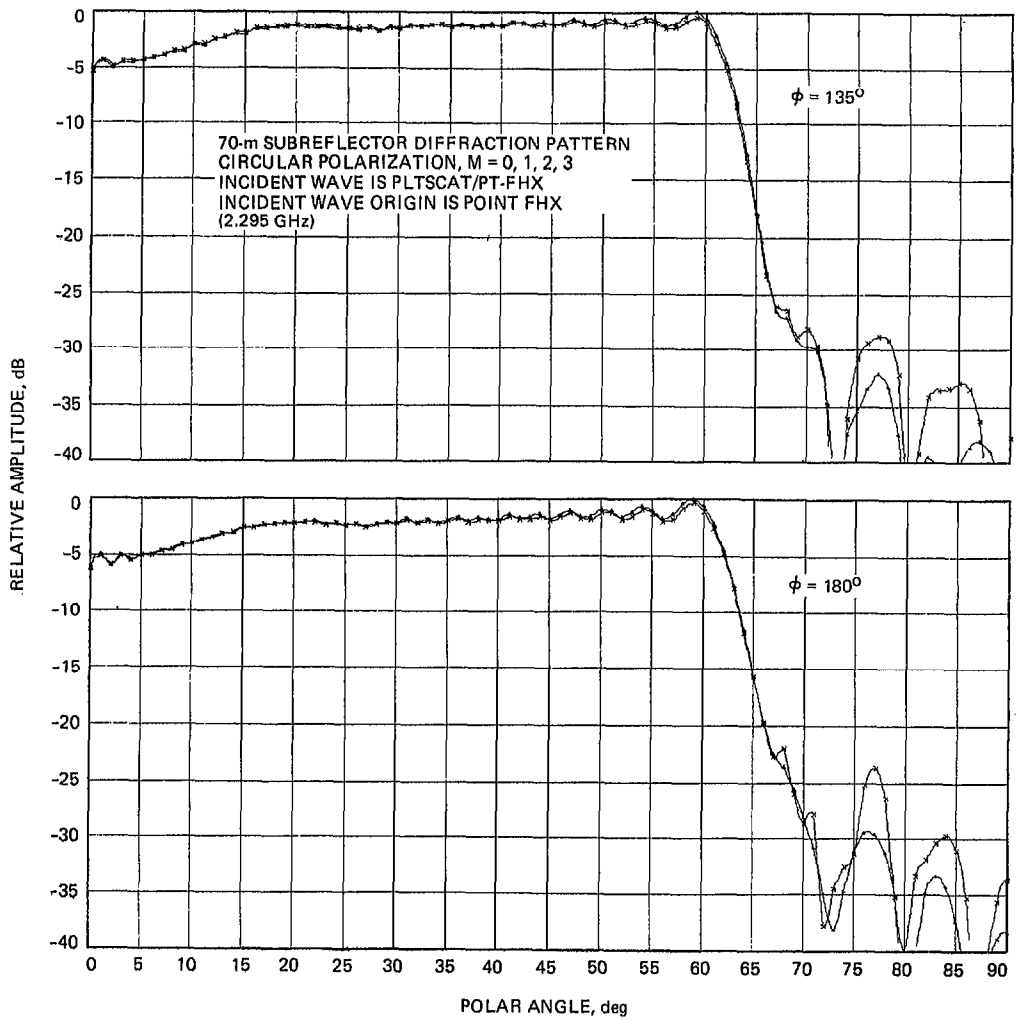
70-m SUBREFLECTOR DIFFRACTION PATTERN
CIRCULAR POLARIZATION, M = 0, 1, 2, 3
INCIDENT WAVE IS PLTSCAT/PT-FHX
INCIDENT WAVE ORIGIN IS POINT FHX
(2.295 GHz)
ϕ = 135°
ϕ = 180°
RELATIVE AMPLITUDE, dB
POLAR ANGLE, deg
0
-5
-10
-15
-20
-25
-30
-35
-40
0 5 10 15 20 25 30 35 40 45 50 55 60 65 70 75 80 85 90

Fig. 4 (contd)

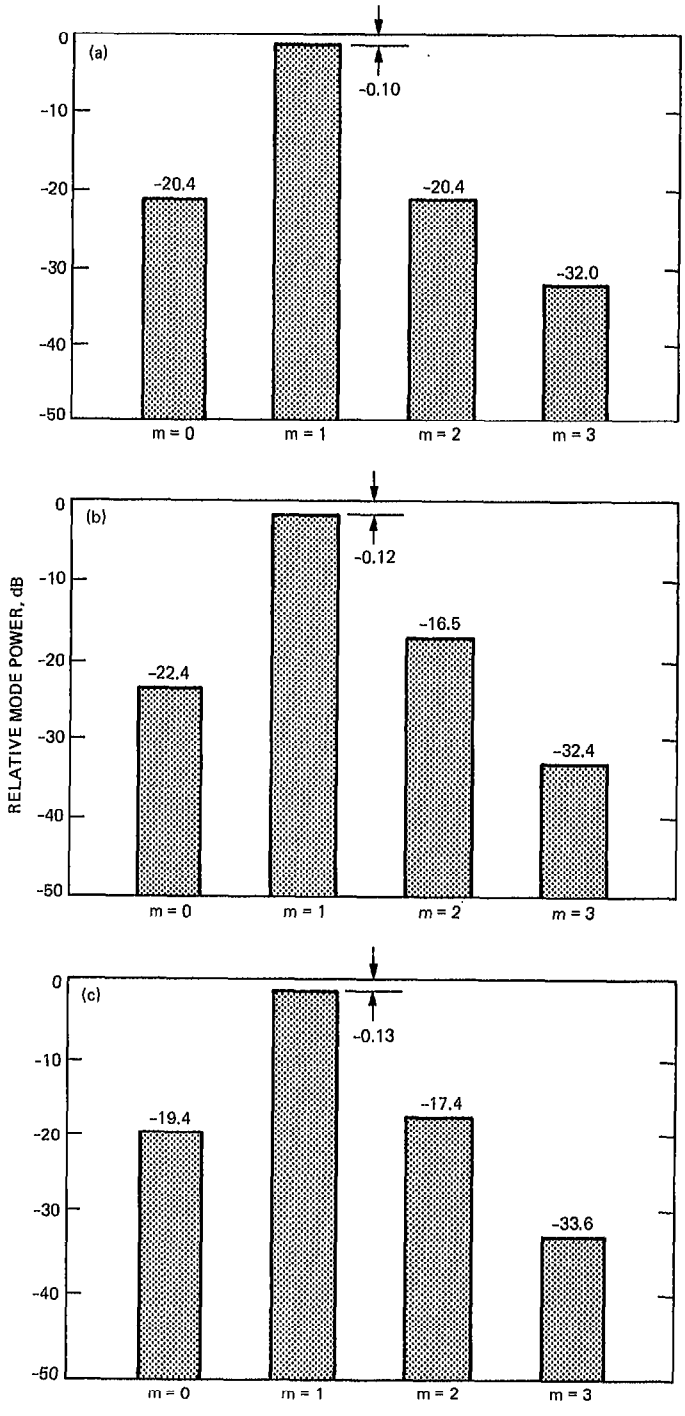

Fig. 5. Azimuthal Fourier mode power content: (a) ellipsoid diffraction pattern; (b) 64-m hyperboloid diffraction pattern; (c) 70-m shaped subreflector diffraction pattern

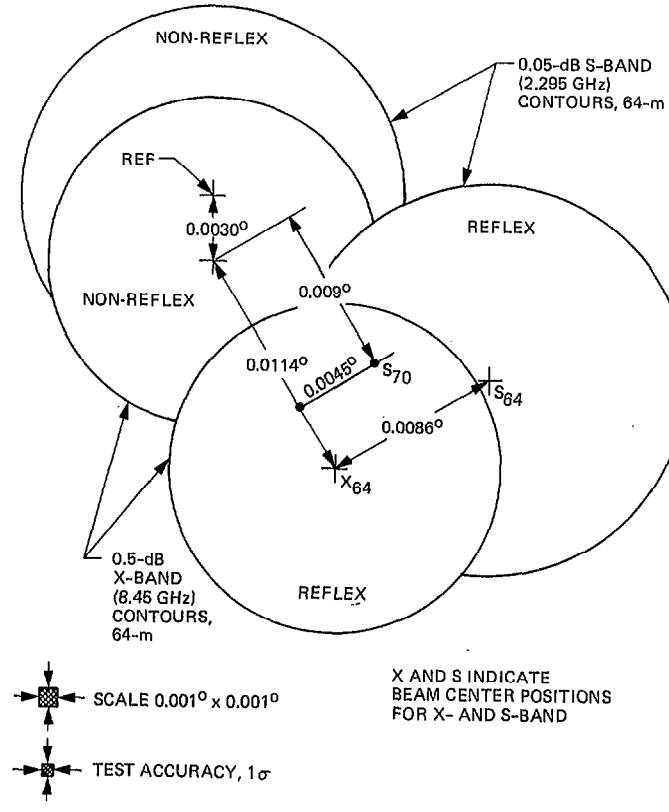

Fig. 6. Predicted S- and X-band beam positions for 70-m antenna

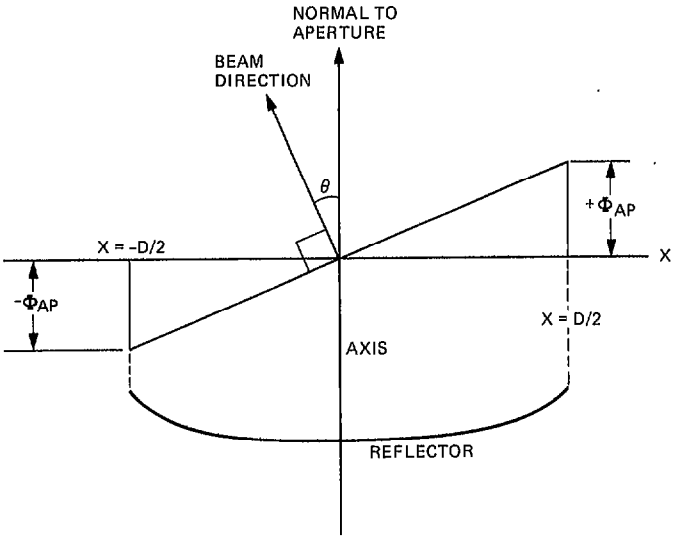

Fig. 7. Beam offset due to linear aperture phase deviation

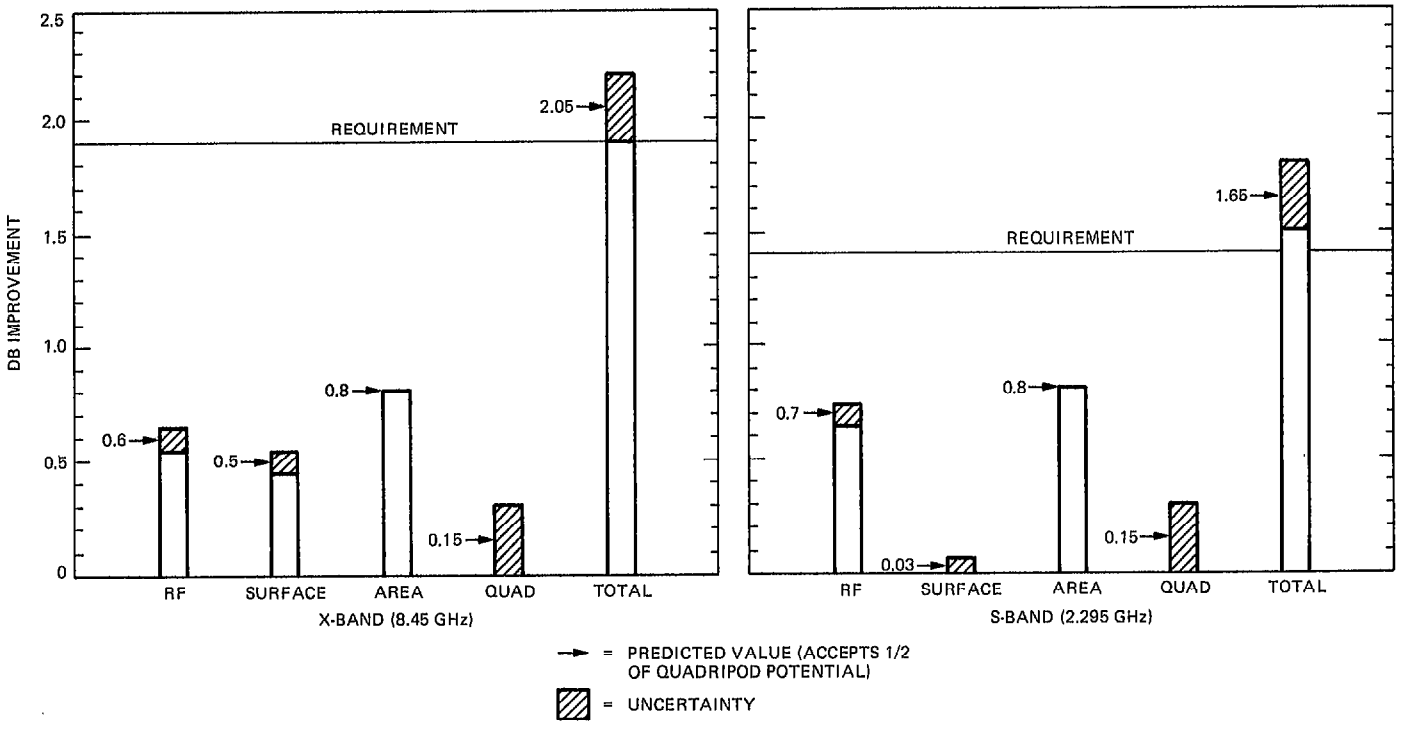

Fig. 8. 70-m antenna reflex feed performance